Supporting information

# Probing the radiative electromagnetic local density of states in nanostructures with a scanning tunneling microscope

Authors: Shuiyan Cao, Mario Zapata-Hererra, Alfredo Campos, Eric Le Moal, Sylvie Marguet, Gérald Dujardin, Mathieu Kociak, Javier Aizpurua, Andrei G. Borisov, and Elizabeth Boer-Duchemin

14 pages, 9 figures

# Supporting Information: Probing the radiative electromagnetic local density of states in nanostructures with a scanning tunneling microscope

Shuiyan Cao,[†,‡,@] Mario Zapata-Herrera,[¶,§,@] Alfredo Campos,[‖,⊥] Eric Le Moal,[‡] Sylvie Marguet,[#] Gérald Dujardin,[‡] Mathieu Kociak,[‖] Javier Aizpurua,[¶] Andrei G. Borisov,[‡] and Elizabeth Boer-Duchemin[*,‡]

†*Department of Applied Physics, Nanjing University of Aeronautics and Astronautics, Nanjing, China*

‡*Université Paris-Saclay, CNRS, Institut des Sciences Moléculaires d'Orsay (ISMO), 91405 Orsay, France*

¶*Materials Physics Center CSIC-UPV/EHU and Donostia International Physics Center DIPC, 20018 Donostia-San Sebastián, Spain*

§*Present address: CIC nanoGUNE, 20018 Donostia-San Sebastián, Spain and Universidad Distrital Francisco José de Caldas, Bogotá, Colombia*

‖*Université Paris-Saclay, CNRS, Laboratoire de Physique des Solides (LPS), France*

⊥*Present address: Facultad de Ciencias y Tecnología, Universidad Tecnológica de Panamá*

#*Université Paris-Saclay, CEA, CNRS, NIMBE, CEA Saclay, Gif-sur-Yvette, France*

@*Contributed equally to this work*

E-mail: Elizabeth.Boer-Duchemin@u-psud.fr

# S1 Calculated spectra and tip effects

In the STM-nanosource experiment, the tungsten STM tip (typical radius $\sim$ 35 nm) is located at a distance on the order of a nanometer from the sample. The point-like vertical oscillating dipole which represents the excitation in the calculation is thus located in a very confined space in the direction perpendicular to the surface. It would thus seem likely that the presence of the tip would affect the spectra. In order to evaluate this effect the following calculations have been performed.

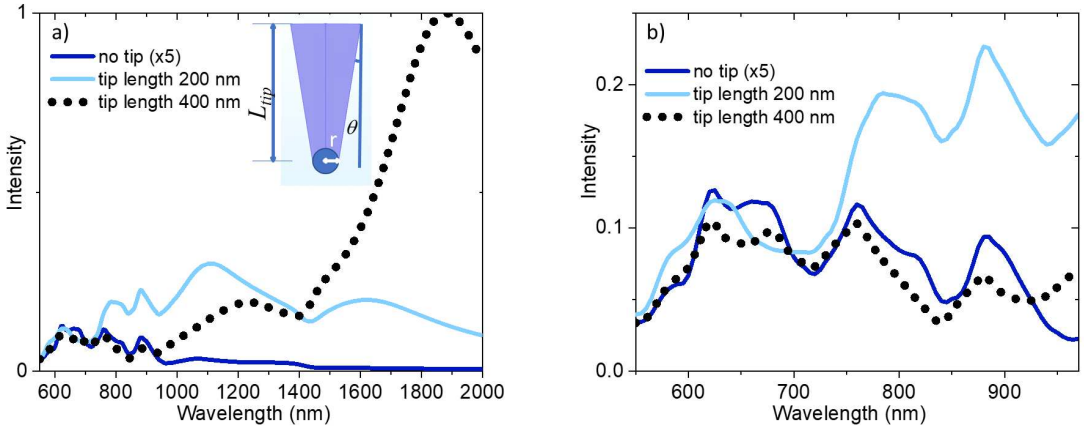


Figure S1: Calculated spectra showing the effect of the length of the tip used in the calculation. The data in (b) is the same as in (a) but only the data in the wavelength range of the experimental results is shown. The radius of the tip is $r = 20$ nm, the triangle side length is 650 nm and the data has been normalized with respect to the highest peak. The result acquired without including a tip is multiplied by a factor of 5. The substrate is represented by a disk of radius 1600 nm and of thickness 200 nm (index of refraction is 2), with air above and below.

The inset of Figure S1 shows the form of the tip used. The end is approximated by a sphere which continues as a cone with an opening angle of $\theta = \tan^{-1}(\frac{1}{6})$. Tip lengths $L_{tip}$ of 200 and 400 nm and radii $r$ of 20 and 40 nm are considered.

Figure S1a shows the calculation of the extended spectra for a dipole excitation in the center of the upper facet of a triangle of side length 650 nm without a tip (dark blue curve), with a tip of length 200 nm (light blue curve) and with a tip of length 400 nm (dotted

black curve). The first thing to note is that while tungsten is not metallic optically speaking at short wavelengths (i.e., the real part of the dielectric function is positive), it becomes plasmonic at longer wavelengths (i.e., the real part of the dielectric function is negative). Thus, as expected, the effect of the tip becomes more important at longer wavelengths. Indeed, the resonance associated with the tip shifts to longer wavelengths as the tip length is increased[1] (note that the "real" tip is several millimeters long). In Figure S1b (which is the same data as Figure S1a but plotted on a different scale), we see that if the tip length is taken to be too short, the relative intensities of the modes in the wavelength range of interest are affected by the tip resonance, but if the tip is long enough, the tip effect on the spectra is negligible—the presence of the tip simply amplifies the intensity (by a factor of 5 in this particular case) without changing significantly the shape or relative intensities of the peaks.

Another possible artifact from the experiment that may be tested with calculations is the effect of an asymmetric tip or local protrusion on the sample. In this case, the tunneling current may not flow from the apex of the tip but from a point on the side. To test the effect of such an asymmetry, the following calculation is carried out: the vertical oscillating dipole representing the excitation remains in position and the tip is shifted a small amount (10 nm) laterally (see Figure S2a). The results of this calculation with an "asymmetric" excitation are shown in Figure S2b in comparison with the usual "symmetric" excitation (i.e., no lateral shift of the tip in the calculation). Here we see that the effect of this possible artifact is again just a difference of intensity, and that the position and relative intensities of the peaks remain unchanged.

A further issue to address is whether the tip produces any artifacts in the results when located next to the edge of the platelet. When the tip is near the edge of the triangle, tunneling current might flow from the side of the particle to the tip (see Figure S3b). In this case, the inelastic tunneling current excitation is best approximated by a *tilted* dipole[2,3] in the direction of the shortest distance between the tip and particle, since the tunneling current decreases exponentially with tip-sample separation.

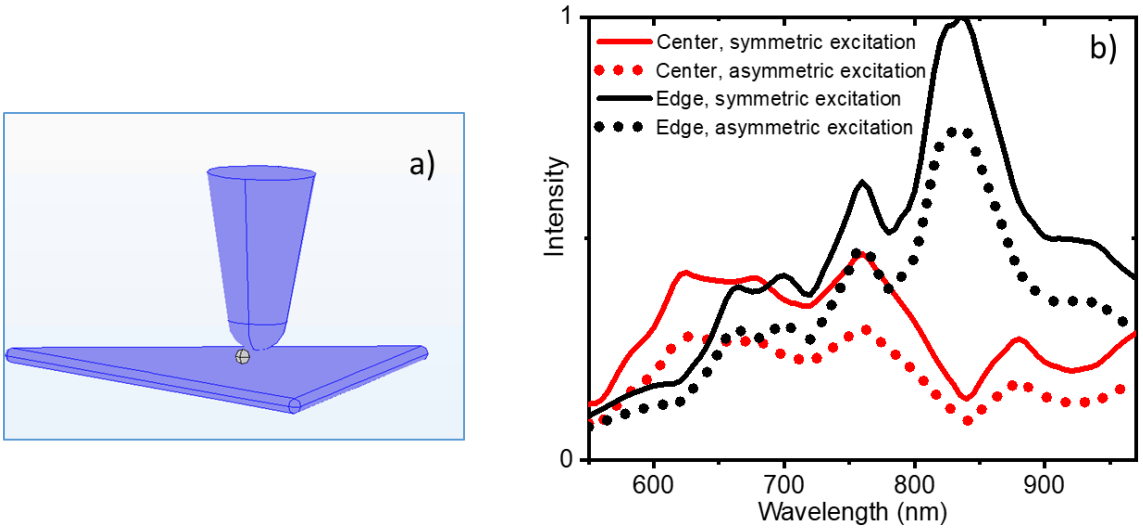


Figure S2: Calculated spectra showing the effect of a possible asymmetry of the tip or of a local protrusion on the sample. (a) Geometry used for the "asymmetric" calculation. The tip is shifted 10 nm laterally with respect to the vertical oscillating dipole representing the excitation (here seen as a small sphere). The radius of the tip is 40 nm and its length is 400 nm. The triangle side length is 650 nm. (b) Calculated spectra for an excitation located in the center of the top face of the triangle (red curves) or on an edge (black curves) for both the usual "symmetric" excitation (continuous curves) and for an "asymmetric" excitation represented by a shift of the tip in the calculation (dotted curves). The effect of the asymmetry is simply a reduction in intensity. The curves of panel b have been normalized with respect to the highest peak. The substrate is represented by a disk of radius 1600 nm and of thickness 200 nm (index of refraction is 2), with air above and below.

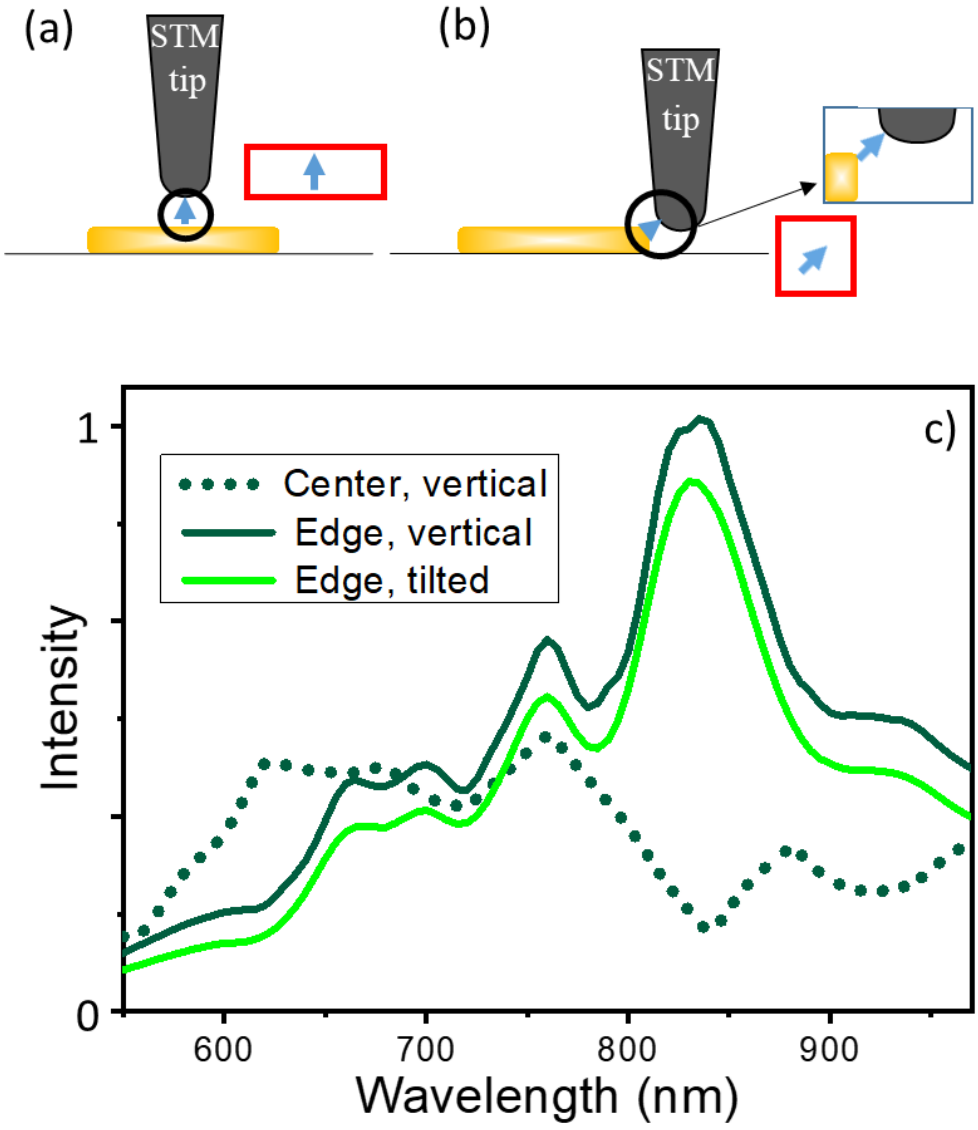


Figure S3: Calculation with the excitation represented as a vertical and as a 'tilted' dipole. The triangle side length is $L = 650$ nm and the tip parameters are $r = 40$ nm and $L_{tip} = 400$ nm. The substrate is represented by a disk of radius 1600 nm and of thickness 200 nm (index of refraction is 2), with air above and below.

Figures S3 a and b show schematically why the case of a *tilted* dipole excitation should be considered in certain cases. When the STM tip is over the center of the triangular platelet, the direction of the tunneling current is perpendicular to the sample surface, and it seems appropriate to approximate the excitation with a vertically-oriented dipole. When the tip is past the edge, however, the current may flow at a diagonal between the tip and triangle, in which case it would seem that the excitation should be represented by a 'tilted' dipole, i.e., one that is oriented at an angle with respect to the normal to the substrate surface. Thus, in order to see the effect of the excitation with a 'tilted' dipole, the spectra is calculated with a dipole oriented at 45°.

The results of these calculations are shown in Figure S3c for an excitation on the edge of the triangle. Here it may be noted that the effect of the tilt is simply to decrease the signal. Thus we may conclude that our experimental data is robust and not affected spectrally by an 'edge effect'.

## S2 STM-nanosource mapping experiments

In a mapping experiment, the STM scans the particle under study in constant current mode ($I_{set-point}$ = 0.1 nA and $V$ = 2.8 V). At each pixel in the scan, the topography, tunneling current, and number of photons emitted into the substrate into the collection angle of the objective are recorded. The photodetector is an avalanche photodiode in front of which different bandpass filters are placed so that wavelength-dependent maps may be obtained. Figure S4 shows two sets of mapping results. In Figure S4a to c, simultaneously-acquired topography, current and photon images for a wavelength of 750 nm are shown, while Figure S4d to f shows the same but for a wavelength of 900 nm. In both the topography and current images there is a local increase in the signal along the edges of the nanoparticle. The same local increase in signal is observed in the photon maps at both wavelengths. Indeed, when there is more total current, more inelastic tunneling current is also expected and thus

more emitted photons should be emitted. Thus in order to obtain meaningful data, the photon images of Figure S4 are divided by their corresponding current images to produce Figure 3a and b of of the main text.

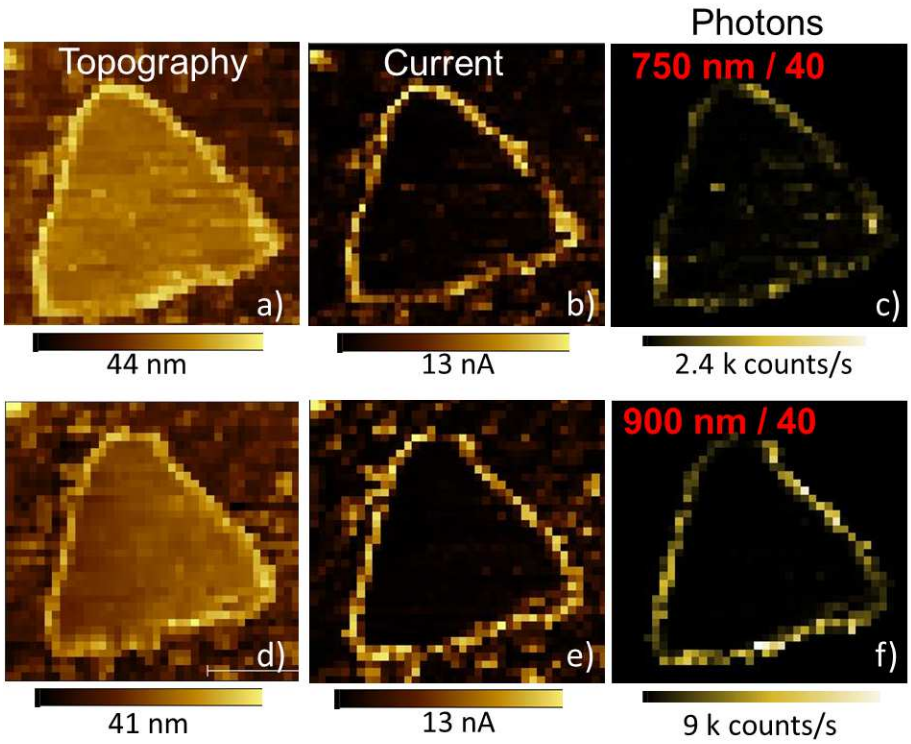


Figure S4: STM mapping results. (a) and (d) Topography, (b) and (e) current and (c) and (f) photon images acquired with (a)-(c) a 750/40 nm or (d)-(f) a 900/40 nm bandpass filter in front of the avalanche photodiode (APD). While the STM scans the particle ($I_{set-point}$ = 0.1 nA and $V = 2.8$ V), the topography and tunneling current are measured, and the resulting emission is detected at each pixel through the transparent substrate by the APD. Triangle side length $L$ is about 630 nm.

## S3 Electron energy loss spectroscopy: position-dependent spectra and spatially resolved maps

Figure S5 shows supplemental results from the electron energy loss spectroscopy (EELS) measurements. The inset to Figure S5a is a high-angle annular dark field image of a $\sim$ 630 nm triangle platelet (thickness $\sim$ 20 nm), showing the five "regions of interest", over which the

signal is integrated to produce the spectra shown in the graph. As for the case of STM-excitation and the calculations (see Figure 2a and Figure 5a of the main text), the position and number of peaks are excitation position dependent. Panels b to e of the figure are spatially resolved EELS maps acquired for the energy ranges shown by the colored rectangles in Figure S5a, or equivalently for the wavelength ranges denoted on each map (e.g., 669-827 nm for Figure S5b). The same tendencies as were seen for the STM-nanosource and simulation results are observed: higher energy modes are most efficiently excited in the center of the top face of the triangle while lower energy modes are most easily excited on the edge.

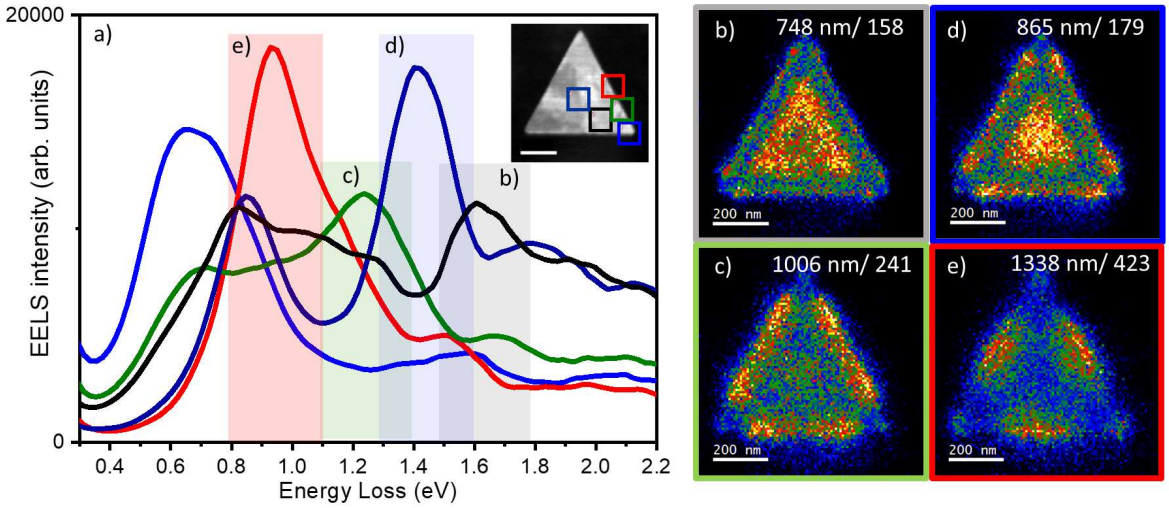


Figure S5: Electron energy loss spectra and maps: The inset in (a) is a high-angle annular dark field (HAADF) image of a gold triangle with a $\sim$ 630 nm side length, showing the regions over which the EEL spectra are integrated. The scale bar in this image is 200 nm. (a) EEL spectra for different excitation positions on the triangle. Note that the same trend is seen as for the STM and simulation results: the most prominent signal is at higher energies when the excitation is in the center of the top face of the triangle, and at lower energies when the excitation is on the edge. Note also the presence of multiple peaks, suggesting the participation of many different modes. (b)-(e) Spatially resolved EELS maps acquired for four different energy ranges. Panels b and c of this figure are the same data as panels c and d of Figure 3 of the main text.

# S4 Spectra as a function of triangle side length: calculation and experiment

Figure S6 shows how the spectra evolve as a function of the triangle side length in both the experiment and calculation. Note that Figure S6b reproduces Figure 5a of the main text. A typical red shift with increasing size (due to the reduction of the restoring force on the induced surface charge with distance) is seen in both cases.[1] Note, however, that this shift is less pronounced for the excitation in the center of the top face, consistent with excited breathing modes.[4,5]

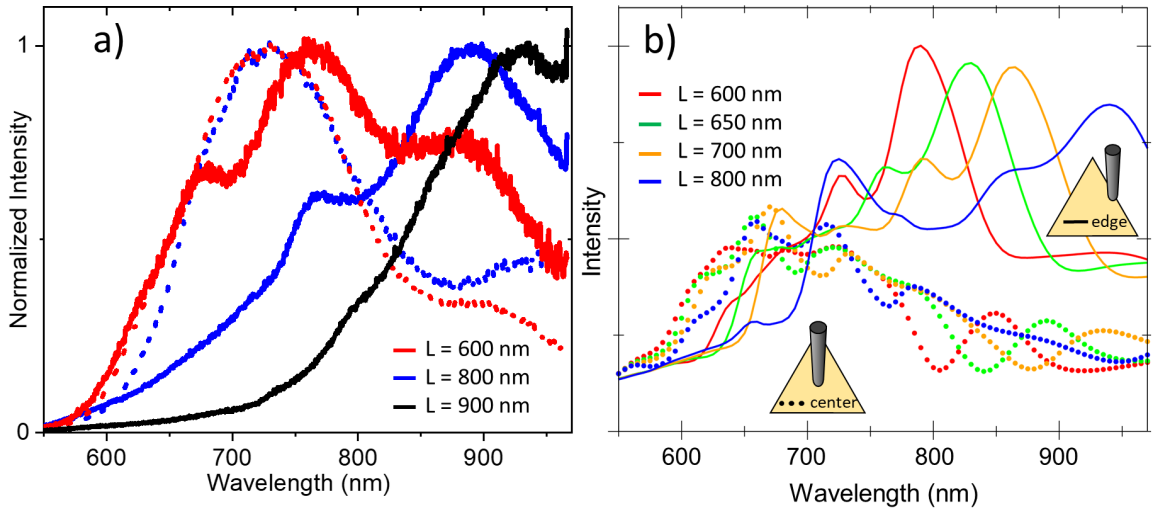


Figure S6: Spectra as a function of triangle side length: experiment and theory. (a) Experimental spectra obtained by placing the STM excitation in the center of the top face of a triangular platelet (dotted curves) or along the triangle edge (continuous curves). Triangle side lengths of $L = 600$, 800, and 900 nm have been investigated. The experimental parameters are sample bias 2.8 V, tunneling current setpoint 0.5 nA, acquisition time 300 s. Each experimental spectrum has been normalized by its maximum value. (b) Calculated spectra obtained by considering the excitation as a vertical oscillating dipole located either in the center of the top face (dotted curves) or on the edge of the triangle (continuous curves). A tip of radius 40 nm and length 400 nm is included in the calculation and the semi-infinite substrate has an index of refraction $n$ =2. Triangle side lengths of $L = 600$, 650, 700 and 800 nm have been investigated. These curves have been normalized with respect to the highest peak in the displayed data range.

Two other remarks may be made regarding the results in Figure S6b. These results have been normalized with respect to the highest peak in the displayed data range. We can conclude that the resulting intensity is higher for excitation on the edge than for excitation in the center of the top face. This is confirmed by the experimental results in Figure 3 of the main text (note that the color scale is about a factor of 5 higher in Figure 3b as compared to Figure 3a in the main article).

The second remark is that we can again easily visualize the general trend observed in the data and confirmed in the simulation: the highest intensity modes for excitation in the center of the top face are found at high energy (short wavelength) while the highest intensity modes for excitation on the edge are at low energy (or long wavelength).

# S5 Comparison of the calculated emission above and below the substrate, and the R-EM-LDOS

As discussed in the main text the *radiative* R-EM-LDOS may be calculated by determining the radiation of a point dipole to the far-field, integrated over a sphere. In the STM-nanosource experiments, however, the emitted light is only collected below the substrate. Is there thus an inherent mis-match between what will be measured in an STM-nanosource experiment and the R-EM-LDOS? This question is answered below.

Figure S7 is produced in the following manner: a vertical oscillating point dipole (flat spectrum) is placed in either the center (position 0) or on the edge (position 2) of a gold triangular platelet ($L$ = 650 nm, thickness 20 nm) on a semi-infinite substrate ($n$ =2). The emission of this dipole to the far-field is then calculated. The continuous curves in Figure S7 are obtained by integrating the out-going energy flux (Poynting vector) over a spherical surface enclosing the entire system. These curves are equivalent to the R-EM-LDOS calculations in Figure 4a and Figure 4b of the main text. The dashed curves in Figure S7 are obtained by integrating the out-going energy flux over only a half-sphere placed

below the surface (i.e., in the substrate), in a manner analogous to the STM-nanosource experiments. Comparing the 'half-space' and 'full-space' calculations, we see that apart from a small change in intensity, the results are equivalent. Thus, the fact that only the light in the substrate is collected in the STM-nanosource experiments does not perturb the measurement of the R-EM-LDOS.

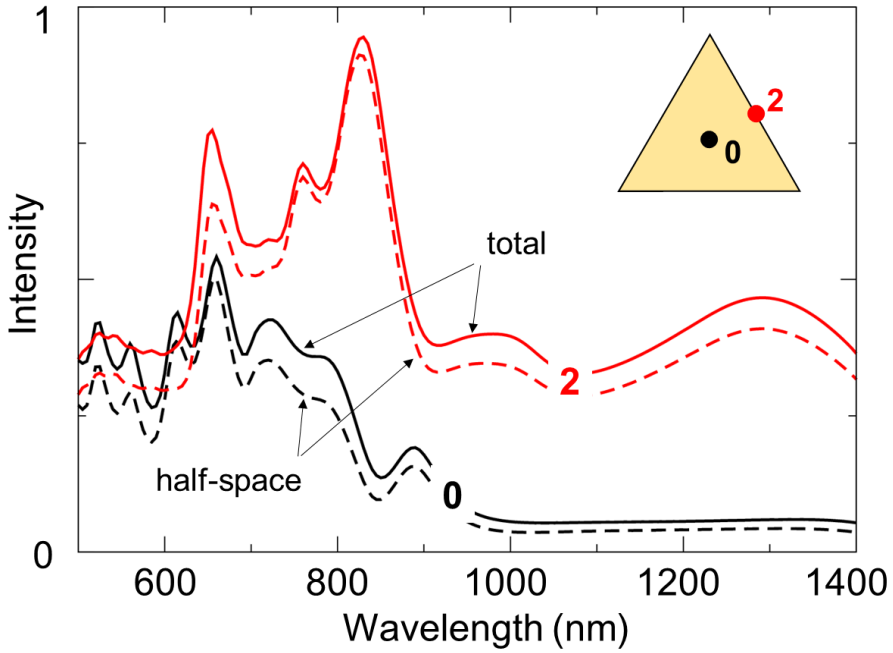


Figure S7: Calculated emitted light to the far-field as a function of wavelength. The continuous curves are obtained for emission in all directions, while the dashed curves are the result for emission into the semi-infinite substrate. The inset shows the two different excitation positions considered.

Next, Figure S8 shows a comparison of the R-EM-LDOS calculations and the calculated photon emission spectra. This figure reproduces the calculated data from Figure 4 and Figure 5 in the main text but now on the same graph for easy comparison. Here we see clearly that for wavelengths greater than 600 nm, the R-EM-LDOS and the calculated spectra have the same variation with wavelength, with slight differences in the the relative intensities of the different peaks. Recall that when calculating the R-EM-LDOS, no STM tip is present, the emission to all-space is considered (i.e., not just to the substrate) and the excitation spectrum is flat. These results again confirm that the collected emission from the STM-nanosource is

equivalent to the R-EM-LDOS for the experimental wavelength range of interest.

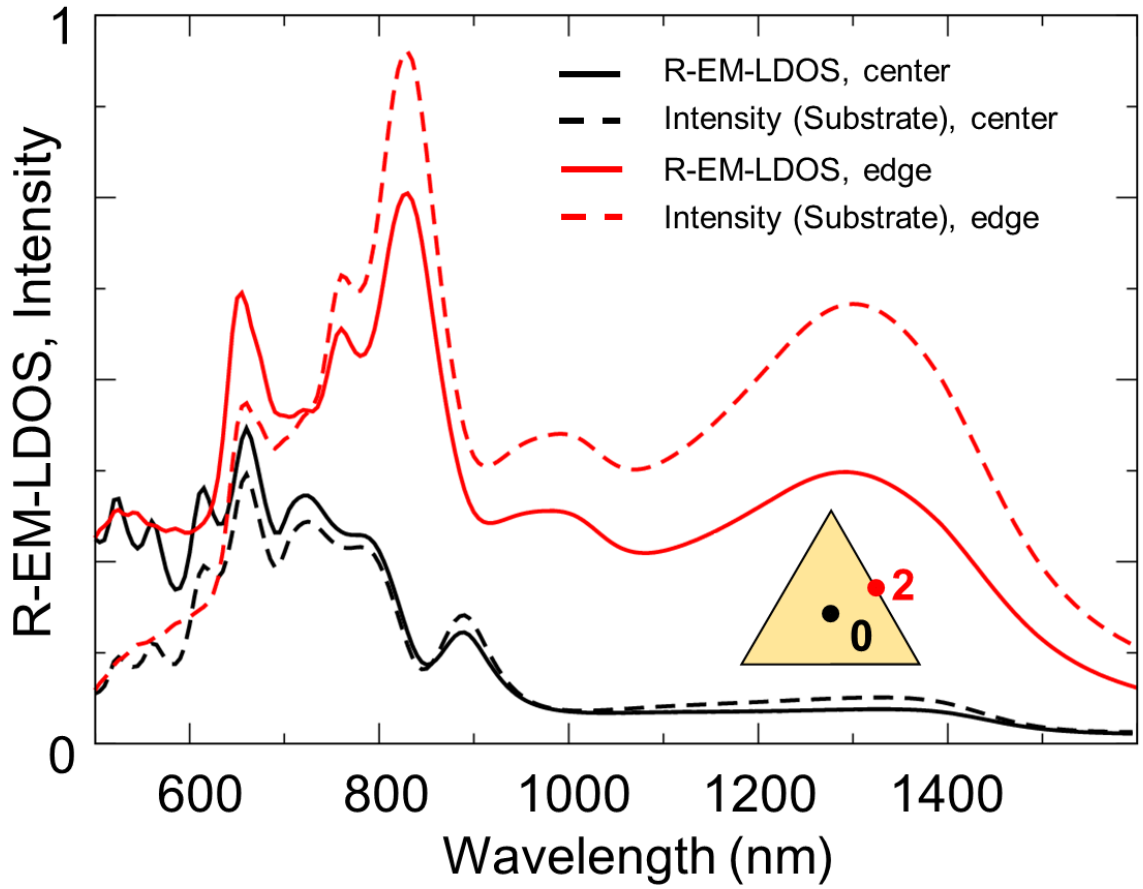


Figure S8: Comparison of the R-EM-LDOS and the calculated photon emission spectra. This figure reproduces the calculated data from Figure 4 and Figure 5 in the main text but now on the same graph for easy comparison.

## S6 Platelet shapes and dimensions: HAADF STEM images

Figure S9 shows high-angle annular dark field (HAADF) scanning transmission electron microscope (STEM) images of four examples of triangular gold platelets. These images clearly show how the experimental system differs from the idealized theoretical one. While a radius of 5 nm for the vertices is taken into account in the calculations, we see in Figure S9c

and Figure S9d that the vertices may be truncated. Another important point to note is that the experimental platelets are never equilateral, contrary to the theoretical assumption. These differences could explain some of the variation observed between the experimental and theoretical results.

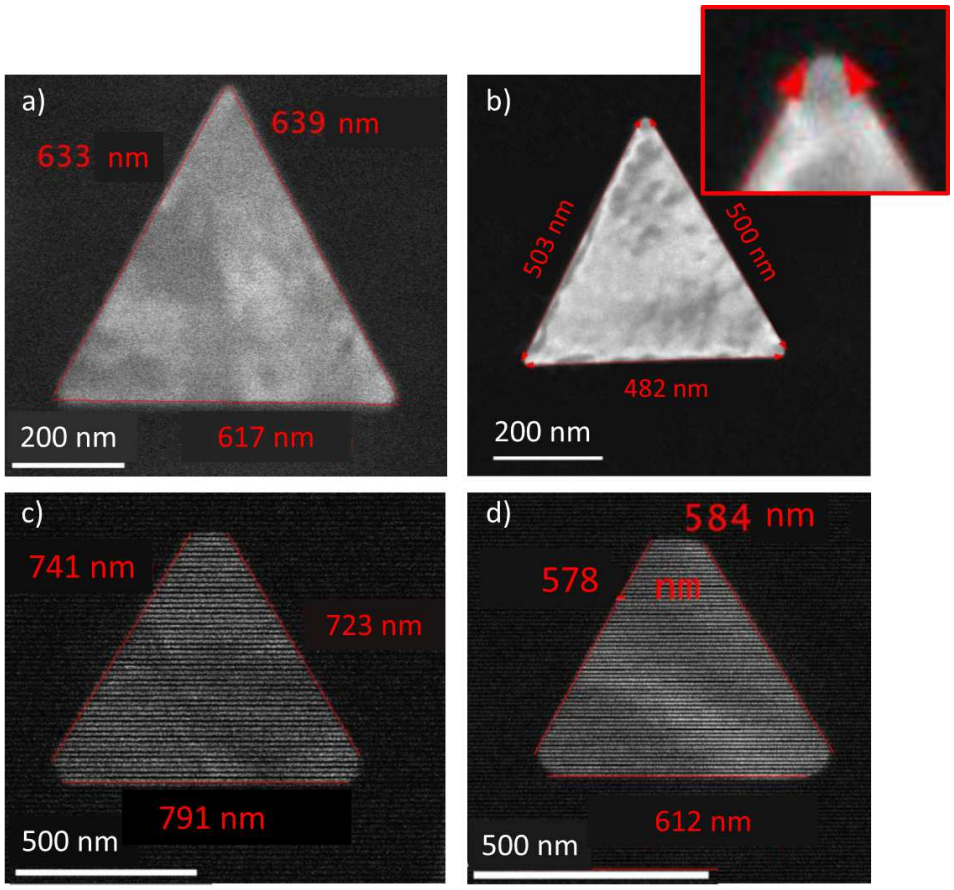


Figure S9: High-angle annular dark field scanning transmission electron microscope images of various triangular gold platelets (thickness 20 nm, lateral dimensions shown in the images). Note that the triangles have rounded vertices (see the inset of panel b) or may also be truncated (panels c and d). Note as well that the triangles are not equilateral. A systematic error of about 10% exists for the lateral measurements while the relative error is much smaller (on the order of $\sim 1\%$).

# References


(1) Kelly, K. L.; Coronado, E.; Zhao, L. L.; Schatz, G. C. The Optical Properties of Metal Nanoparticles: The Influence of Size, Shape, and Dielectric Environment. *J. Phys. Chem. B* **2003**, *107*, 668–677.

(2) Le Moal, E.; Marguet, S.; Rogez, B.; Mukherjee, S.; Dos Santos, P.; Boer-Duchemin, E.; Comtet, G.; Dujardin, G. An electrically excited nanoscale light source with active angular control of the emitted light. *Nano Letters* **2013**, *13*, 4198–205.

(3) Myrach, P.; Nilius, N.; Freund, H.-J. Photon mapping of individual Ag particles on MgO/Mo(001). *Phys. Rev. B* **2011**, *83*, 035416.

(4) Krug, M. K.; Reisecker, M.; Hohenau, A.; Ditlbacher, H.; Truegler, A.; Hohenester, U.; Krenn, J. R. Probing plasmonic breathing modes optically. *Applied Physics Letters* **2014**, *105*, 171103.

(5) Campos, A.; Arbouet, A.; Martin, J.; Gérard, D.; Proust, J.; Plain, J.; Kociak, M. Plasmonic Breathing and Edge Modes in Aluminum Nanotriangles. *ACS Photonics* **2017**, *4*, 1257–1263.